# LUND UNIVERSITY

**Detailed Heat Release Analyses With Regard To Combustion of RME and Oxygenated Fuels in an HSDI Diesel Engine**

Horn, Uwe; Egnell, Rolf; Andersson, Öivind; Johansson, Bengt

*Published in:*
CI Engine Performance for Use with Alternative Fuels

2007

[Link to publication](#)

Total number of authors:
4

# Detailed Heat Release Analyses With Regard To Combustion of RME and Oxygenated Fuels in an HSDI Diesel Engine

**Uwe Horn, Rolf Egnell and Bengt Johansson**
Lund Institute of Technology

**Öivind Andersson**
Volvo Car Corporation

## ABSTRACT

Experiments on a modern DI Diesel engine were carried out: The engine was fuelled with standard Diesel fuel, RME and a mixture of 85% standard Diesel fuel, 5% RME and 10% higher alcohols under low load conditions (4 bar IMEP).

During these experiments, different external EGR levels were applied while the injection timing was chosen in a way to keep the location of 50% heat release constant.

Emission analysis results were in accordance with widely known correlations: Increasing EGR rates lowered NOx emissions. This is explained by a decrease of global air-fuel ratio entailing longer ignition delay. Local gas-fuel ratio increases during ignition delay and local combustion temperature is lowered. Exhaust gas analysis indicated further a strong increase of CO, PM and unburned HC emissions at high EGR levels. This resulted in lower combustion efficiency. PM emissions however, decreased above 50% EGR which was also in accordance with previously reported results.

Besides those similar trends, fuel dependent differences in indicated thermal efficiency as well as CO, HC, NOx and especially PM emissions were observed.

These differences were evaluated by detailed heat release analysis and explanation models based upon fuel characteristics as fuel viscosity and fuel distillation curve.

Fuel spray evaporation and heat release were influenced by these fuel characteristics. Due to these characteristics it was concluded that RME has a higher tendency to form fuel rich zones at low load conditions than the other tested fuel types.

Moreover it was found that improved fuel spray vaporisation is an option to improve exhaust emissions at low load conditions.

## INTRODUCTION

In the degree that costs and demand of crude oil rise, diminish the economical disadvantages for alternative Diesel fuels, resulting in a variety of feasible substitutes. Both the Diesel itself engine and its fuel have been developed concurrently since a long time and reached a level of sophistication that makes it hard for alternative Diesel fuels to compete.

Many fuel substitutes have been shown to have deviating exhaust emissions from conventional fuel. The methyl ester of rapeseed oil (known as RME/biodiesel) is receiving increasing attention as an alternative fuel for Diesel engines. RME is a non-toxic, biodegradable and renewable fuel with the potential to reduce engine exhaust emissions [3]. Differences to petroleum based Diesel fuel are a slightly increased cetane number, low sulphur content, low amount of aromatics, lower volatility and a short distillation temperature interval. This has both positive and negative effects on exhaust emissions:

- The $CO_2$ neutrality of RME is one of the most common arguments propagating the use RME instead of standard Diesel fuel. If the economically most worthwhile fuel (i.e. tax reduced standard Diesel fuel for the agriculture sector) is used for production of RME, $CO_2$ neutrality is allayed somewhat.

- During ECE tests it has previously been observed that Diesel engines fuelled with RME emit a lower amount of unburned hydrocarbon (HC) and carbon monoxide (CO) emissions decrease compared to standard Euro Diesel fuel (EDF) whereas NOx emissions are slightly increased. At high engine loads particulate matter (*PM*) is reported to be on the same level or slightly lower as for standard Diesel fuels and at a higher level under low load conditions. [6, 12]

- It has also been reported that engines fuelled with RME produce a higher fraction of soluble organic material in exhaust PM compared to engine run with EDF. However, during ECE tests, PM is lowered if the engine is fuelled with RME. Non-regulated emissions as aromatic hydrocarbons and specific alkenes are reported to be considerably lower with RME. Aldehydes and ketones are reported to be on the same level as for standard Diesel fuels. [1, 6]

- In addition, the mutagenicity of RME emissions is low compared to fossil fuels indicating a reduced health risk from cancer which is related to the extremely low sulphur content of RME [10]. Low exhaust gas sulphur content reduces moreover catalyst wear due to sulphate formation [1, 2]. New conventional Diesel fuels (DF) provide also low sulphur contents (Euro-DF <50 *ppm*, City-DF <10 *ppm*) and are most likely on their way to match the sulphur content of RME (<5 *ppm*) [13].

Today's Diesel engines' electronic control units (ECU) are adapted to a certain amount of fuel energy per volume. If the engine is fuelled with RME which has a lower heating value (LHV) that is 12% reduced compared to standard Diesel fuel, the engine control unit interprets the higher fuel mass flow as a higher engine power output level. Injection timing, turbo charging and EGR are adjusted for this virtually higher power level but not for the real engine operating point [5].

The main disadvantage for RME is its vaporisation and self ignition characteristics at low load conditions. Hence, engine experiments were carried out at 4 bar IMEP with Euro Diesel fuel as reference, RME and a mixture of 85% EDF, 10% higher alcohols and 5% RME (AGRO15). During these engine experiments EGR and injection pressure were varied. As a result differences in exhaust emissions due to EGR, injection pressure and fuel type were observed (see Figure 5 and Figure 6).

The objective of this work was to find answers for fuel dependent differences in thermal efficiency and exhaust gas emissions. As combustion and emission formation of alternative fuels have not been fundamentally explained yet [16], a detailed analysis approach based on explanation models for fuel characteristics was chosen to explain these observed differences.

A more detailed impression on the interdependency between combustion characteristics and fuel properties is given in the following sections:

**COMBUSTION CHARACTERISTICS**

At low load conditions, the main part of combustion is premixed since only a small amount of fuel is injected which vaporises and mixes during ignition delay. Premixed combustion rate is limited by the chemical reaction rate. Due to low local reaction temperatures, incomplete combustion products as CO and HC are left.

However, even under low load conditions diffusive combustion occurs. Reaction rates of mixture controlled combustion are low compared to reaction rates of premixed combustion. As chemical reactions are mixing controlled, time scales for fuel spray/cylinder gas interaction differ in order of magnitudes from the time scales of branching reactions. Chemical reactions occur under high local temperatures at so called "hot spots" with local $\frac{A}{F}$ ratio close to stoichiometry. These hot reaction zones consume already vaporised fuel and products remaining from premixed combustion and are considered as the main source for thermal NOx if the local $\frac{A}{F}$ ratio is sufficiently high [4,11].

As long as a liquid fuel phase is existent during combustion (i.e. fuel injected close to start of combustion (SOC) or during combustion), a part of the released heat is used to vaporise the liquid fuel fraction. These vaporisation zones are fuel rich. During diffusive combustion under fuel rich conditions and local temperatures about 1800 K, clusters of carbon agglomerates are formed. These carbon clusters consist basically of polycyclic aromatic hydrocarbons (PAH) as well as amorphous, partially peroxidised carbon, so called soot. These carbon agglomerates are consumed by diffusive combustion under globally lean conditions [5 pg.10]. The duration of this lean, diffusive combustion interval with locally high temperatures is important for oxidation of combustion residuals, especially PM.

Fuel that is injected after SOC is consumed by diffusive combustion if enough local oxygen and heat energy for ignition is available. Increased ambient pressures and gas temperatures during premixed combustion lower ignition delay for the fuel fraction injected during this phase.

Diffusive combustion is controlled by the amount of locally available oxygen. At high EGR levels, combustion of fuel fractions injected at late stage is quenched due to increased cylinder charge mass entrainment after a long ignition delay. Local reaction temperatures decrease due to the lack of locally available oxygen. Hence, oxidation of combustion residuals (i.e. HC, CO, PM) during diffusive combustion at high EGR levels is poor and results into increased exhaust emissions. The behaviour of PM emissions due to increased EGR level is depicted in Figure 1:
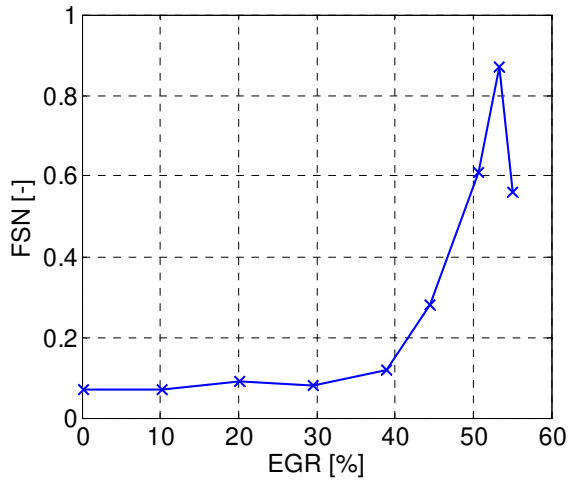
**Figure 1: Influence of intake EGR level on PM emissions**



**Figure 2: Indicators for premixed and diffusive diesel combustion (40% EGR)**

Ignition delay increases with increasing EGR level. If all fuel is injected well before *SOC* (see Figure 1 – highest EGR level), no diffusive combustion occurs at all due to a sufficiently long ignition delay. Due to stronger mass entrainment into the fuel spray, local temperatures are below 1500 K, which is the lower limit for soot formation. Hence, PM emissions are reduced and remaining residuals after premixed combustion are not oxidised due to the lack of diffusive combustion. This entails increased HC and CO emissions (Figure 5 – maximum EGR). As the length of ignition delay is highly dependent on fuel mixture generation, the timing of *SOC* becomes hard to control and results in increased variations in maximum cylinder pressure as well as IMEP.

Even premixed reaction speed is reduced with increasing EGR levels which is due to the lack of locally available oxygen. This effect contributes to an improved mixing of fuel mass with cylinder charge mass during combustion. Emerging diffusive "hot spots" can distribute their heat to a larger amount of charge mass. In this way local temperatures are lowered and NOx formation is reduced, which was reflected in emission measurements (Figure 5).

As the equilibrium of the NOx reactions is dependent on the local oxygen concentration, decreasing local oxygen concentration shifts the reaction equilibrium in a way that NOx output is lowered (Figure 5 - NOx).

Late stage premixed combustion shifts gradually to increasing diffusive combustion with decreasing EGR level. Both combustion types overlay each other, which makes it hard to find an indicator for the start of diffusive combustion.

The heat release rate (HRR) and the 2$^{nd}$ heat release derivate (*D2HR*) were used to characterise the ratio of premixed and diffusive combustion. This characterisation is explained for the 40% EGR case in Figure 2:
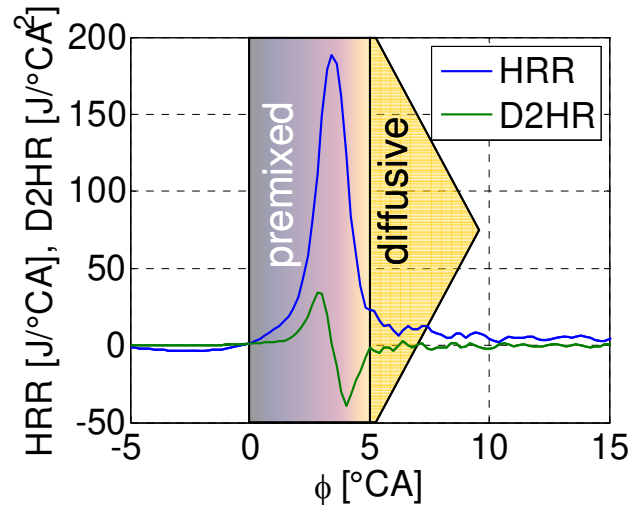
The "start" of diffusive-only combustion is indicated by a slope change of HRR and D2HR. If the amount of diffusive HR shall be estimated from the HRR curve, errors in estimation of the start of diffusive combustion are crucial due to the strong HRR during premixed combustion: An estimation error of ±0.2°CA within the premixed phase yields a difference in HR ratio of ~5%.
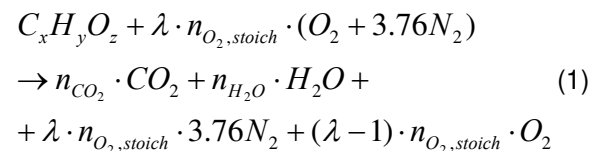
For the characteristics of partially premixed combustion, the following is summarised:

- The amount of EGR has a major influence on ignition delay and combustion duration.

- Fuel/air mixture generation is considerably influenced by ignition delay.

- Exhaust emissions (i.e. CO, HC and PM) are considerably affected when diffusive combustion shifts to premixed-only combustion.

- Local reaction temperature and oxygen concentration are the major factors influencing NOx formation.

**FUEL CHARACTERISTICS**

OXYGENATES

The global reaction equilibrium is influenced by combustion of oxygenated fuels in the following way:

$$C_xH_yO_z + \lambda \cdot n_{O_2,stoich} \cdot (O_2 + 3.76N_2)$$
$$\rightarrow n_{CO_2} \cdot CO_2 + n_{H_2O} \cdot H_2O + \qquad (1)$$
$$+ \lambda \cdot n_{O_2,stoich} \cdot 3.76N_2 + (\lambda - 1) \cdot n_{O_2,stoich} \cdot O_2$$

For oxygenated fuels, a part of the oxygen needed for chemical reactions is already bound in fuel molecules, which has two effects:

- Due to a lower stoichiometric $A/F$ ratio, local cylinder gas entrainment is lower which increases local combustion temperatures.

- The ratio of stoichiometric fuel mass and released fuel energy is higher, which is due to lower fuel energy content. This entails lower local combustion temperatures.

If vaporisation properties are not affected by oxygenates, increased local oxygen concentration might have a higher tendency towards NOx formation whereas PM is lowered due to improved oxidation properties. This effect, however, might be compensated by the higher amount of fuel mass needed to release a certain amount of energy.

## SAUTER MEAN DIAMETER

Spray vaporisation properties for RME deviate considerably from EDF. This is due to increased fuel viscosity and surface tension which entails larger average droplet size. A measure for the average droplet size is the Sauter Mean Diameter (SMD) [15]:

$$SMD = C \cdot \left( \frac{\mu_f \cdot \sqrt{(\omega/\rho)_f}}{\rho_g \cdot u_g^2} \right)^{2/3} \qquad (2)$$

SMD is related to the fuel viscosity $\mu_f$ [Pa s], fuel surface tension $\omega_g$ [N/m], fuel density $\rho_f$ [kg/m³], cylinder charge density $\rho_g$ [kg/m³] and the velocity difference between fuel and cylinder charge $u_g$ [m/s]. The empiric SMD relation is scaled by the correction factor $C$ to fit to measurement results.

The velocity difference $u_g$ is highly dependent on injection pressure; it is presumed that SMD is considerably influenced by increasing injection pressure (see Figure 19).

Calculation results for the SMD show how fuel properties influence the average droplet size at 500 bar injection pressure. (Table 1):

**Table 1: Influence of Fuel Properties on droplet size**

| Fuel Type | SMD (at 500 bar) |
|-----------|------------------|
| EDF | 46 $\mu$m |
| AGRO15 | 46 $\mu$m |
| RME | 84 $\mu$m |

Apart from injection pressure fuel viscosity has the strongest influence on SMD. Fuel dependent differences in viscosity (see Appendix Table 5) are hence reflected in SMD.
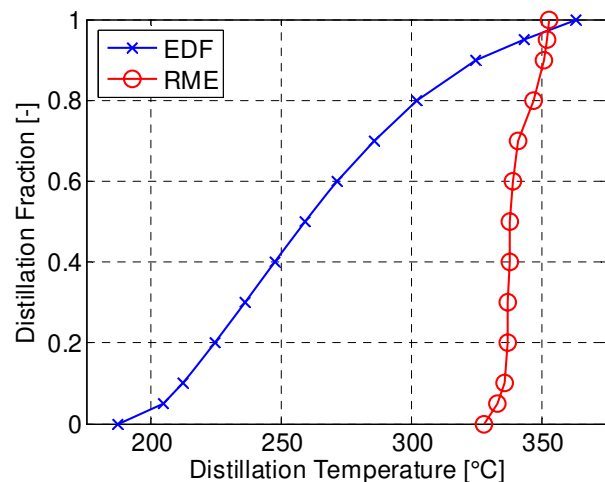
## DISTILLATION CURVE

The fuel distillation middle temperature (T50) for pure fuel components like n-alkanes and aromates, is an indicator for the average molecule size. Hence, T50 is a good indicator for fuel CN. Aromates are reported to have a somewhat less distinct relation between T50 and CN. A high amount of fuel additives changes overall fuel CN considerably and makes it hard to estimate standard fuel CN from T50 [5].

The most important fuel characteristics besides the fuel cetane number (CN) are described by the shape of the distillation curve: The cetane number of the fuel fraction vaporising during the start of the distillation curve has an influence on exhaust emissions: A higher initial fuel cetane number (ICN) decreases ignition delay. Hence, both PM and NOx-emissions are lower with ICN improvers even though the overall fuel cetane number is virtually unaffected [17].

A flat distillation curve is advantageous due to a lower fuel evaporation rate over the whole distillation temperature interval. It has been reported that thermal engine efficiency increases slightly due to a better controlled vaporized fuel supply during the whole combustion process [5].

Even though the CN for RME is slightly higher than for EDF, combustion properties are reported to be poor at low load conditions [1,5,12]. This is due to the composition of RME. RME consists of a few types of acid ethyl esters with similar properties whereas EDF consists of 200 different hydrocarbon types with varying properties. Hence, RME can be considered as a virtually pure substance with a very high distillation curve gradient (cf. Figure 3):



**Figure 3: Distillation curve for EDF and RME**

The distillation middle temperature T50 as well as strong distillation temperature gradient cause HC, CO and PM emissions. Especially under low load and cold start conditions HC emissions are produced by incomplete combustion due to poorly controlled fuel vaporisation as

a result of a high T50 and a short distillation temperature interval.

The initial vaporised fuel fraction is considered to have a major influence on ignition delay. Thus, a high boiling point increases ignition delay as more time is needed to vaporise the initial fuel fraction.

In contrary to EDF, fuel compounds with PM precursors (i.e. polycyclic aromatic hydrocarbons – PAH) are not included in RME. From this aspect, the affinity for RME to form PM is lower due to the lack of PAH in the molecular structure but is most likely countervailed by its poor evaporation characteristics.

For distillation curve characteristics, the following is concluded:

- A high distillation middle temperature (T50) is considered to increase ignition delay due to delayed fuel evaporation.

- A high distillation curve gradient is assumed to increase the affinity to form fuel rich zones as fuel is distributed under a shorter temperature interval.

For the differences in fuel characteristics between EDF, AGRO15 and RME, the following is summarised:

- EDF (certification fuel) was chosen as the reference fuel. It contains ignition delay improvers with comparatively low ICN and oxidation characteristics are improved by a low volatile fuel fraction with high FCN.

- AGRO15 consists of 85% EDF and has thus similar combustion characteristics as EDF. The fuel fraction of 10% higher alcohols (i.e. oxygenates) might have a positive influence on oxidation characteristics.

- For RME, fuel properties as viscosity, heat capacity, boiling point, distillation curve, lower volatility and chemical structure are more different from EDF. This means that formation and growth of particulates during combustion as well as oxidation characteristics might differ considerably. The fuel oxygen content of RME might compensate increased emission formation due to high fuel evaporation rates when reaching the boiling point.

## MEASUREMENT SETUP

The experiments discussed in this article were carried out with a single cylinder research engine. Cylinder head, engine piston, and common rail (CR) injection system of a Volvo D5 HSDI Diesel engine with the following specifications were used:

**Table 2: Engine specifications**

| Cylinder Head type | Volvo D5 |
|---|---|
| Bore | 81 mm |
| Stroke | 92.3 mm |
| Displacement | 480 cm$^3$ |
| Compression Ratio $r_{c,stat}$ | 16.15:1 |
| Injection Cone Angle | 139° |
| Injector Type | solenoid |
| Injection Nozzle Hole (Number x Diameter) | 7x0.14 mm |

The test rig was equipped with an adjustable EGR system and miscellaneous sensors. The most important sensors for analysis and interpretation of measuring results are depicted in the following figure:
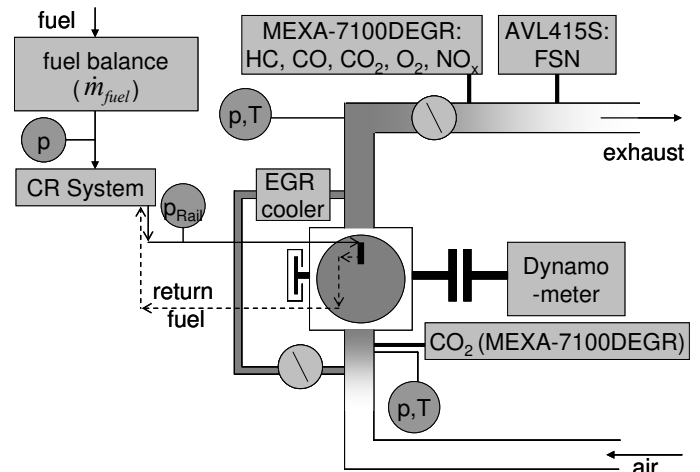


**Figure 4: Engine setup and location of measuring points**

Smoke emissions (in the unit filter smoke number – FSN) were measured with a device (*AVL415S*) that derived exhaust gas particle concentration from the blackening of filter paper that was exposed to the exhaust gas flow for a certain duration. Fuel effects on particle properties as particle size distribution, solubility or carcinogenic components can not be analyzed adequately with this measuring technique [6]. This technique however is a commonly used measuring method and in accordance with today's emission tests that focus on overall particle mass.

Exhaust gases were measured with an exhaust gas analyser (*HORIBA MEXA-7100DEGR*) NOx and HC emissions were measured at a temperature of 191°C. NOx emissions were measured with a chemiluminescence analyser (CLA-755A) whereas HC emission measurements were done by means of a flame ionization analyser from Horiba (*FIA-725A*). FIA results could be erroneous due to fuel dependent differences in the molecular structure of unburned hydrocarbons.
Intake gas, end exhaust $O_2$, CO and $CO_2$ sample gases were dehumidified before measurement. The EGR rate was calculated from intake and exhaust gas $CO_2$ concentration:

$$\chi_{EGR} = \frac{\chi_{CO_2,in}}{\chi_{CO_2,out}} \qquad (3)$$

For Diesel combustion the major fuel dependent differences in exhaust emissions are observed at low load conditions [5]. Hence, the following test conditions were chosen:

Table 3: Engine test conditions

| Engine speed | 1200 rpm |
|---|---|
| IMEP | ~4 bar |
| Inlet temperature | 105 °C |
| Inlet pressure | 1.05 bar |
| Rail pressure | 500 bar |
| Fuel Consumption (FC): | |
| $FC_{EDF}$ | 0.119 g/s |
| $FC_{RME}$ | 0.129 g/s |
| $FC_{AGRO15}$ | 0.120 g/s |

Fuelling rate was constant for each fuel. It was adjusted for differences in density and heating value in order to inject the same energy amount for all fuels (Table 3).

Cylinder pressure was measured with a piezoelectric pressure sensor (*Kistler 6056*) with sample every 0.2°CA. Both, fast and slow measurement data were averaged from 200 engine cycles.

## MEASUREMENTS

Figure 5 shows how emissions changed during variation of EGR under constant fuelling rate. Fuel specific differences in indicated mean effective pressure of the combustion phase (IMEP$_{gross}$) and exhaust emissions were observed:
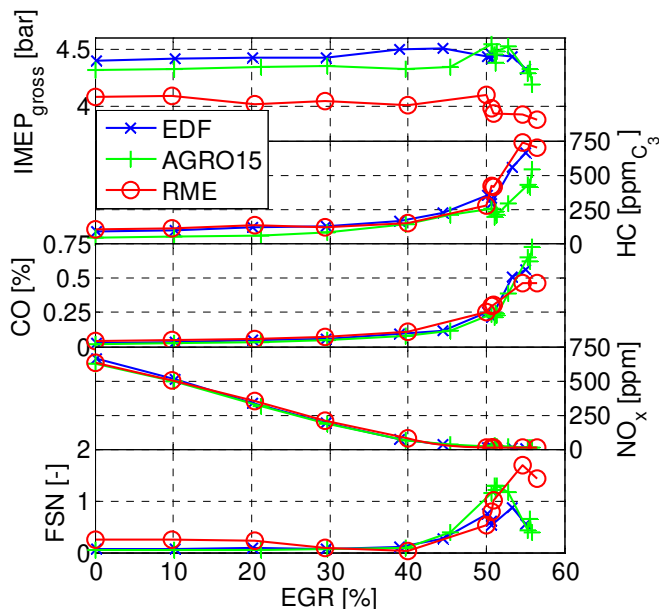


Figure 5: Exhaust emissions vs. EGR for three different fuels

Compared to the reference fuel EDF AGRO15 showed slightly improved HC, CO and PM emissions at low EGR conditions whereas these emissions where slightly increased for the RME case (Figure 5). Exhaust emissions for all fuel types converged with increasing EGR level. Compared to EDF, NOx emissions were slightly lower for both RME and AGRO15.

HC, CO, and PM emissions increased considerably with high EGR levels, which was due to incomplete combustion (see section *Combustion Characteristics*), NOx emissions were close to detection limit which was due to low temperature combustion.

To estimate the influence of injection pressure on mixture generation, a rail pressure variation at the point of maximum PM emission (i.e. ~50% EGR) was conducted (Figure 6). Changes in exhaust gas emissions were observed:
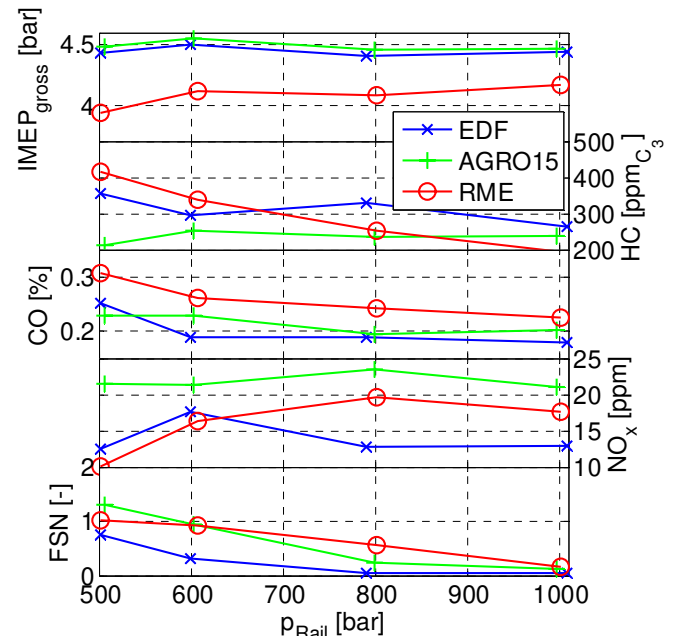


Figure 6: Influence of rail pressure on engine load exhaust emissions (50% EGR)

Higher local $A/F$ ratio during premixed combustion influenced the trade off between particle generation and oxidation in a way that PM output was lowered. Increasing injection pressure at 50% EGR, PM could be reduced for all fuels. HC and CO emissions were improved for the RME case while exhaust emissions for AGRO15 and EDF were within measurement accuracy.

The observed emission characteristics led to the following assumptions:

- NOx and PM measurements indicate more fuel rich combustion for the RME case compared to the EDF case.

- The choice of higher alcohols in AGRO15 improves oxidation characteristics which is reflected in the amount of unburned hydrocarbons (HC).

- PM output is influenced by the trade off between PM generation and PM oxidation. Both mechanisms are dependent on local oxygen concentration, local temperature and residence time. If injection pressure is increased, gas entrainment before ignition and even during combustion is improved entailing higher local oxygen concentrations. Due to lower PM formation at higher local $A/F$ ratio and improved particle oxidation characteristics, PM emissions are improved, especially for the RME case.

To be able to verify these assumptions, a detailed analysis approach was chosen to analyse differences in emission and combustion characteristics due to fuel properties.

## ANALYSIS METHODOLOGY

For being able to investigate how calculated heat release (HR) was dependent on fuel property differences, a HR analysis approach was chosen which took changes in cylinder gas composition into account.

The gas composition model based upon the apparent heat release rate HRR$_{net}$ which was derived from the 1$^{st}$ law equation:

$$HRR_{net} = \frac{\kappa}{\kappa - 1} pdV + \frac{1}{\kappa - 1} Vdp \qquad (4)$$

$\kappa$ is the adiabatic exponent, $p$ the cylinder pressure and $V$ the crank angle dependent cylinder volume. For the heat release analysis the following assumptions were made:

- The analysis is restricted to a control volume during the closed valve period (IVC-EVO). Blow-by is not considered.
- The control volume is assumed to be a perfectly stirred reactor.
- Cylinder pressure is assumed to be uniform in the whole control volume.
- The initial gas temperature at IVC was resolved from the inlet gas temperature.
- The cylinder mass at IVC was calculated from the average mole mass of cylinder gas composition and the amount of moles at IVC, which was derived from the amount of injected fuel mass, the exhaust gas oxygen concentration, the EGR concentration and residual gases.
- The amount of residual gases is calculated by the ideal gas law at TDC during gas exchange phase.
- The level of external EGR is calculated from intake and exhaust gas $CO_2$ measurement.

- Convective heat transfer between gases and the cylinder wall was estimated by Woschni's correlation.
- The cylinder volume was divided into two regions: One with unburned fuel-air mixture and one with burned exhaust gas.
- The crank angle dependent cylinder gas composition was calculated from a normalised HR curve and global chemical reaction.
- Heat transfer between those two reaction zones was neglected.
- The cylinder wall temperature was assumed to be constant within the analysis interval.

## EFFECTIVE COMPRESSION RATIO

The effective compression ratio ($r_{c,eff}$) is different from the static compression ratio ($r_{c,stat}$) due to measuring errors of the static compression volume and elastic strain in engine components during engine run. An estimation error in $r_{c,eff}$ shifts the phasing of calculated HR, which induces analysis errors.

For a motored pressure curve, a compression interval $\Delta\phi$ closely after IVC is chosen, where cylinder wall temperature is close to the global gas temperature. By assuming a realistic $\kappa$ for the considered gas temperature, the effective compression ratio is calculated by adiabatic compression. The effective compression ratio $r_{c,eff}$ is varied by means of the correlations $V_{clearance} = \frac{V_{displacement}}{(r_c - 1)}$ and $V = V_{clearance} + V_{displacement}$ in such a way that the *HR* for the considered interval is minimised:

$$HRR(\Delta\phi) = \frac{\kappa}{\kappa - 1} p_1 \cdot (\Delta V) + \frac{1}{\kappa - 1} V_1 \cdot (\Delta p) \qquad (5)$$
$$HR(\Delta\phi) \to 0$$

If $r_{c,eff}$ is estimated for a motored pressure curve, realistic assumption for the change of the adiabatic exponent $\kappa$ due to cylinder gas composition can be done.

## CHANGE OF ADIABATIC EXPONENT

The adiabatic exponent (also called ratio of specific heats) $\kappa = \overline{C}_P / \overline{C}_V$ is used to describe adiabatic changes of intensive gas state variables. Using the relation $\overline{C}_P = \overline{C}_V + R_u$, one yields $\kappa = (\overline{C}_V + R_u)/\overline{C}_V$. Hence, an increase of intake gas heat capacity lowers $\kappa$. The increase of exhaust gas heat capacity compared to intake gas heat capacity is to be explained with its dependency on the molecular degree of freedom (DOF): Gas molecules have different DOF (translation, rotation

and oscillation modes) which are dependent on their molecular structure. These different modes are successively activated with higher temperatures. At extremely high temperatures, even more heat can be stored due to effects such as dissociation and ionisation [14].

At standard conditions, the adiabatic coefficient of air can be calculated from the molecular DOF to $\kappa = 1.4$ which is very close to its literature value [14, pg. 514ff]. If intake air is mixed with warm exhaust gas, the amount of carbon dioxide and water molecules increases. Those molecules have a considerably higher heat capacity than nitrogen and oxygen molecules.

Assuming $\kappa$ being constant and independent of cylinder gas composition changes during combustion, a rough mean value for the whole combustion cycle between $\kappa = 1.4$ (air at $T \approx 300K$) and $\kappa = 1.3$ (exhaust gas at $T \approx 650K, \lambda = 1$) can be chosen.

The following figure shows the sensitivity of maximum HRR for different values of $\kappa$:
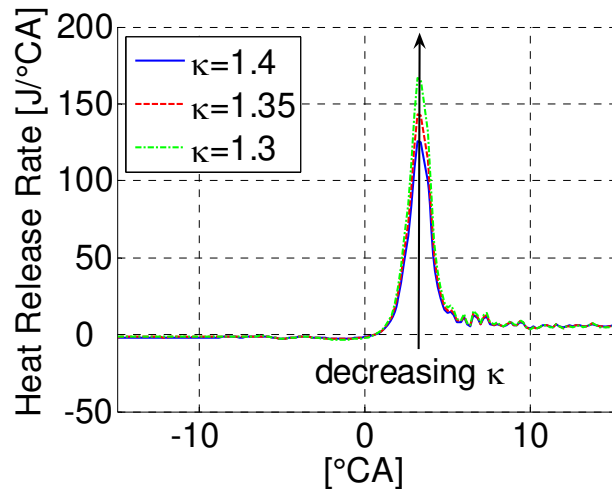


**Figure 7: Influence of changes in constant adiabatic exponent on rate of heat release**

A low adiabatic exponent increases the calculated HRR since more energy can be stored in a control volume at a given temperature. Due to the higher molecular DOF, the specific heat capacity of the cylinder gas increases concurrently with the intake gas EGR level. Hence, underestimation of $\kappa$ entails a higher overall HR. Since the HR calculation error is larger at high HRR, the calculated HR is not only erroneous in amplitude but also in phasing. Hence, it is important to make realistic assumptions for $\kappa$ if the HR is used to characterise combustion phenomena under use of excessive EGR.

A robust method to estimate the change in $\kappa$ due to cylinder gas composition at IVC is to assume adiabatic compression within a compression interval shortly after IVC (Figure 8).
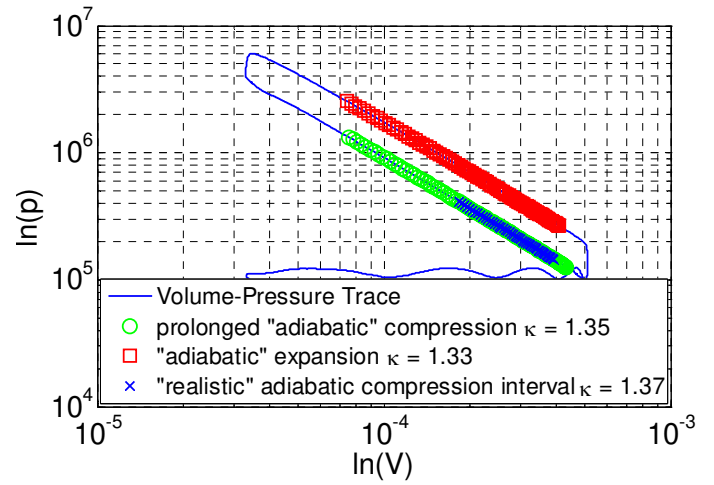


**Figure 8: Influence of choice of interval on $\kappa$ calculation**

A "realistic" adiabatic compression interval is chosen for cylinder gas temperatures close to the cylinder wall temperature. In this compression interval, changes in $\kappa$ due to heat losses can be neglected. The slope of the ln-p-V-diagram represents the adiabatic exponent $\kappa$ and can be calculated by:

$$\kappa_{IVC} = \frac{\ln(p_1 / p_2)}{\ln(V_2 / V_1)} \qquad (6)$$

The subscripts $1$ and $2$ indicate start and end of the adiabatic compression interval. If the "adiabatic" compression interval is prolonged until fuel injection, $\kappa$ changes arbitrarily due to cylinder wall heat losses.

The change of cylinder gas composition due to combustion can be taken into account by assuming adiabatic expansion during the expansion stroke after the end of combustion. Even here, heat losses to the cylinder walls are included in the adiabatic exponent. The difference in $\kappa$ between compression and expansion stroke (Figure 8 – *circle* and *square*) is interpolated linearly or with a previously calculated normalised HR.

The adiabatic exponent is highly temperature dependent due to the change in DOF of the cylinder gas molecules. This temperature dependency was modelled with an exponential approach:

$$\kappa(T) = \kappa_0 - k_1 \exp(-k_2 / T) \qquad (7)$$

$\kappa_0$ is a reference value for the intake gas, T is the actual ambient gas temperature, $k_{1,2}$ are model constants. It has previously been shown, that this temperature model yields sufficiently exact results compared to results from a multi zone HR model [4]. However, deviations in $\kappa$ due to cylinder gas compositions are not considered. Thus, the $\kappa$-temperature-model was scaled with respect to the cylinder gas composition. The deviation in $\kappa$ due to change of cylinder gas composition during combustion is depicted in Figure 9.
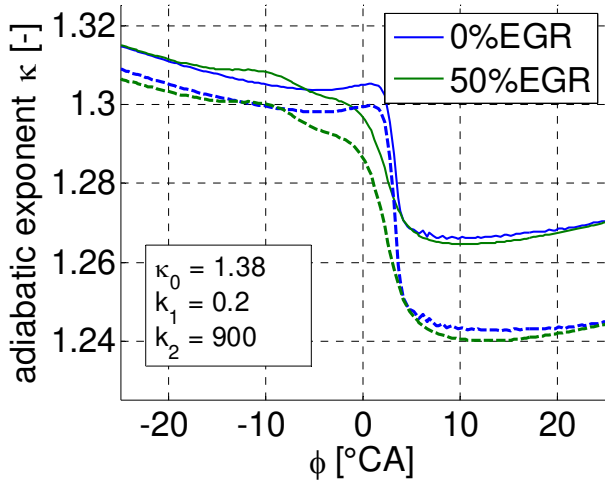
**Figure 9: Temperature and Gas Composition-Model for κ at different EGR levels**

The response of the temperature-model (eq.7) on ambient cylinder gas temperature is plotted as a continuous line. The dashed lines show the $\kappa$-value that was fitted to the crank angle dependent cylinder gas composition by calculating an averaged adiabatic exponent from the cylinder pressure trace until and after combustion (see Figure 8). Changes in cylinder gas composition due to combustion were considered by interpolating $\kappa_{compression}$ and $\kappa_{expansion}$ with a previously calculated normalized HR. The calculated adiabatic exponent (*dashed lines*) is lower than the result of the temperature model because a fraction of cylinder wall heat losses are accounted as increased cylinder gas heat capacity. Thus, the $\kappa$ model used during HR-analysis yields a higher amount of released heat than the temperature model only.

Ignition Delay and Injection Timing

The injection process is indicated by a local minimum in the HRR before SOC and is due to heat losses during fuel evaporation. Hence, the start of this local minimum was defined as start of injection (SOI).

The injection duration DOI was derived from the 1st law equation. Assuming that the hydrodynamic pressure equals the pressure difference between injection nozzle $p_{inj}$ and combustion chamber $p_{cyl}$ during injection, the injection velocity $c_{inj}$ can be estimated by Bernoulli's law:

$$p_{inj} - p_{cyl} = \rho_{fuel} \cdot \frac{c_{inj}^2}{2} \qquad (8)$$

The injection mass flow rate is calculated from the injection velocity, a hole dependent discharge coefficient $C_{d,holes}$ and the nozzle hole area $A_{holes}$:

$$\dot{m}_{inj} = \rho \cdot c_{inj} \cdot C_{d,holes} \cdot A_{holes} \qquad (9)$$

The overall hole area $A_{holes}$ is calculated as follows:

$$A_{holes} = N_{holes} \cdot \pi \cdot \frac{(corr_D \cdot D_{holes})^2}{4} \qquad (10)$$

with:

- $N_{holes}$ being the number of holes [-]

- $D_{holes}$ being the hole diameter [m]

- $corr_D$ being the hole diameter correction factor [-].

The correction factor was chosen in a way that *DOI* matched to detailed injection simulation results for one reference point.

The discharge coefficient $C_{d,holes}$ is calculated from an empirical equation regarding flow characteristics due to nozzle hole geometry [4]:

$$C_{d,holes} = \begin{cases} \left(1.5 + 13.74 \cdot \sqrt{\dfrac{L}{D \cdot \mathrm{Re}}}\right)^{-0.5} & \text{for } \dfrac{D \cdot \mathrm{Re}}{L} \geq 50 \\ \left(2.28 + 64 \cdot \dfrac{L}{D \cdot \mathrm{Re}}\right)^{-0.5} & \text{for } \dfrac{D \cdot \mathrm{Re}}{L} < 50 \end{cases} \qquad (11)$$

L is the length of the hole [m]

$D$ is the hydraulic diameter of the hole, including the hole diameter correction factor [m]

Re is the Reynolds number, i.e. $\mathrm{Re} = \dfrac{c_{inj} \cdot D}{\nu}$, where:

$c_{inj}$ is the fuel flow speed [m/s]

$\nu$ is the kinematic fuel viscosity [m²/s]

The ignition delay was calculated as the difference between SOC and SOI (Figure 14). If the injection duration (DOI) is added to SOI, one gets an impression of how much fuel is injected after SOC.

Fuel injection after *SOC* (*SOC-EOI < 0*) implies that a fuel fraction is consumed by diffusive combustion instead of premixed combustion. The delay between end of injection (EOI) and *SOC* can be used to estimate injection mass ratio before and after *SOC* (Figure 15). This estimate of injection mass ratio represents an upper limit of the fuel mass that can be consumed by premixed combustion.

## Ambient Gas Temperature

The cylinder gas state is defined by three of the four state variables (p, V, n, T). The ideal gas law states the correlation between these state variables:

$$pV = nR_u T \tag{12}$$

The crank angle dependent cylinder gas temperature is calculated from the gas composition at IVC:

$$\left(\frac{pV}{nT}\right)_{IVC} = \left(\frac{pV}{nT}\right)_{CA} = R_u = const. \tag{13}$$

Knowing the crank angle dependent pressure trace $p_{CA}$, volume $V_{CA}$ and mole number $n_{CA}$, the crank angle dependent global cylinder gas temperature $T_{CA}$ is calculated from (eq. 13):

$$T_{CA} = T_{IVC} \frac{(pV)_{CA}}{(pV)_{IVC}} \frac{n_{IVC}}{n_{CA}} \tag{14}$$

This ambient cylinder gas temperature considers cylinder gas composition during combustion and is typically somewhat lower than ambient gas temperature calculated without influence of cylinder gas composition. This temperature difference influences heat transfer calculation.

## HEAT TRANSFER

Due to the complexity of the flow patterns in the combustion chamber, estimating the heat transfer to the cylinder walls is very difficult. However, various correlations have been derived from measurements to predict the heat transfer coefficient. During this work Woschni's correlation [10] has been used to estimate cylinder wall heat transfer:

$$h = C\left[B^{-0.2} p^{0.8} w^{0.8} T^{-0.53}\right] \tag{15}$$

The constant C was chosen according to Woschni's formulation, $h$ is the heat transfer coefficient, $B$ is a characteristic length which was set equal to the bore diameter in *[m]*, $p$ is the cylinder pressure in *[bar]*, $T$ is the gas temperature in *[K]* and $w$ is the characteristic gas speed in *[m/s]* given below:

$$w = C_1 v_m + C_2 T_{IVC} \frac{V_s}{V_{stroke}} \frac{p - p_0}{p_{IVC}} \tag{16}$$

with:

$$C_1 = 2.28$$

$$C_2 = \begin{cases} 0 & \text{(compression)} \\ 3.24 \cdot 10^{-3} \, m/_{sK} & \text{(expansion)} \end{cases}$$

Reference pressure and temperature were chosen at IVC. $v_m$ is the mean piston speed, $T_{IVC}$ is the reference temperature, $V_s/V_{stroke}$ is the ratio of swept volume and a reference volume (here the stroke volume), $\frac{p - p_0}{p_{IVC}}$ is the ratio of the pressure difference between actual pressure, motored pressure curve and the reference pressure.

High rates of *EGR* entail a considerable change of the compression stroke pressure curve due to the change of $\kappa$. This change in $\kappa$, however is not reflected in a motored pressure.

Hence, the motored pressure curve $p_0$ was estimated from the actual pressure curve until SOI by assuming isentropic compression until *TDC*. The expansion curve was mirrored from the compression curve. Calculation of the pressure difference between compression and expansion stroke of a "real" motored pressure curve (i.e. *without* EGR) indicated a maximum pressure loss of *1 bar* at *20°CA* after *TDC* due to cylinder wall heat losses.

These crank angle dependent pressure losses were subtracted from the expansion curve to minimize estimation error of an EGR dependent motored pressure curve.

## ACCURACY OF MEASUREMENTS AND ANALYSIS

### COMBUSTION PHASING

The amount of EGR was varied while injection timing was adjusted in such a way that the point of 50% HR (CA50) was kept constant. The fast HR analysis program that was used to estimate combustion phasing differed from the HR program used for detailed HR calculation. In Figure 10, an EGR dependent difference in calculated CA50 is observed:
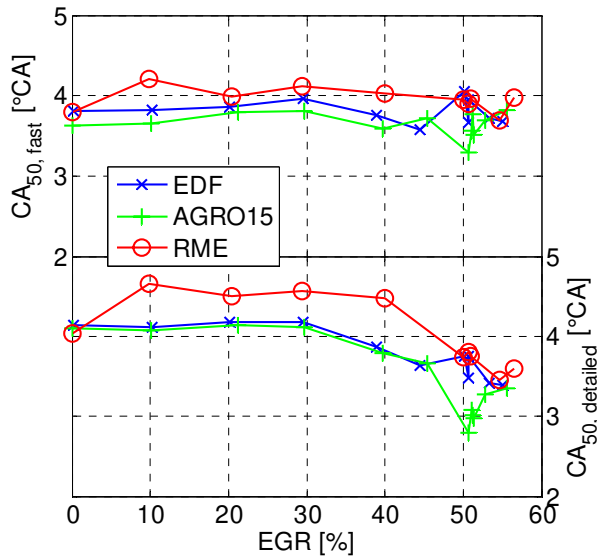
**Figure 10: Differences in combustion phasing due to choice of evaluation model**

At high EGR levels, combustion advanced somewhat closer to TDC. The depicted difference in CA50 due to HR analysis method is related to the following parameters:

**Table 4: Differences in HR analysis parameters**

| Parameter | Fast: $HR_{net}$ | Detailed $HR_{gross}$ |
|---|---|---|
| $\kappa$ | • Constant<br>• Estimated from isentropic compression | • Crank angle dependent<br>• Dependent on cylinder gas composition<br>• Temperature dependent |
| $\kappa$ -**Analysis Interval** | [-110...60]°CA | Compression and expansion cycle |
| **CA50/SOC Estimation Interval** | $[HR_0...HR_{max}]$ | $[HR_{min}...HR_{max}]$ |

Differences in indicated thermal efficiency due to combustion phasing are negligible for the considered variation interval of CA50 (cf. A.3). To improve clarity and comparability, different HRR were synchronised at SOC (see Figure 13).

Determination of SOC however varies dependent on choice of the analysis interval for calculation of mass fraction burnt. If the reference point for determination of SOC is set to the point where the HR exceeds 0 (Table 4 – $HR_0$), one obtains a later *SOC* as if the reference point is set to the minimum HR (Table 4 – $HR_{min}$). SOC shifts due to choice of analysis interval with ~3°CA. As $HR_{min}$ is not influenced by the type of calculated HR (with/without heat losses), this criterion was used to determine SOC during detailed HR calculations.

COMBUSTION EFFICIENCY

A strong increase of CO, PM and unburned HC emissions at EGR levels beyond 40% lowered combustion efficiency ($\eta_C$) considerably:
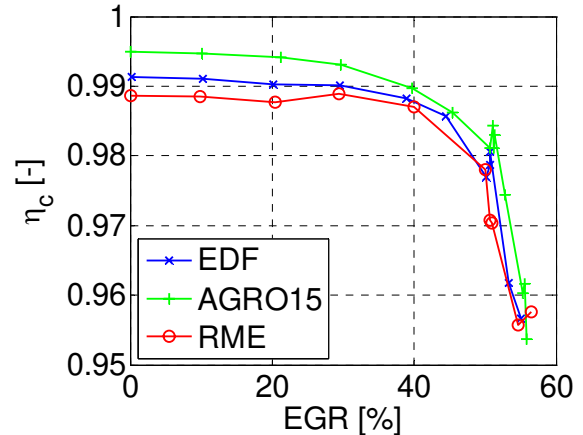


**Figure 11: EGR vs. combustion efficiency $\eta_c$**

The energy content of CO and HC emissions was used to calculate combustion efficiency. Fuel dependent deviations in $\eta_C$ were within an interval of ±0.5%.

Moreover is $\eta_C$ only slightly affected due to the low PM mass flow fraction and heating value. The FID measurement result is dependent on molecular characteristics as molecule length and formation. HC emissions were measured as propane equivalent without any fuel dependent correction factor.

For the calculation of combustion efficiency it can be concluded, that exhaust measurement results and their influence on combustion efficiency have to be considered carefully. The effect of combustion efficiency is investigated more precisely in the following two sections.

ENERGY CONVERSION EFFICIENCY

Energy conversion efficiency $\eta_E$ was calculated as the quotient of the maximum HR ($HR_{gross,max}$) and the supplied energy. The supplied fuel energy was calculated as the product of measured fuel mass flow, LHV and the combustion efficiency $\eta_C$ (see Appendix eq.2).

Dependent on *EGR* level, the maximum HR ($HR_{max}$) varied with *~5%*. By comparing $HR_{max}$ with the amount of released chemical energy, one gets an estimate on the quality of Woschnis empirical equation (Figure 12).
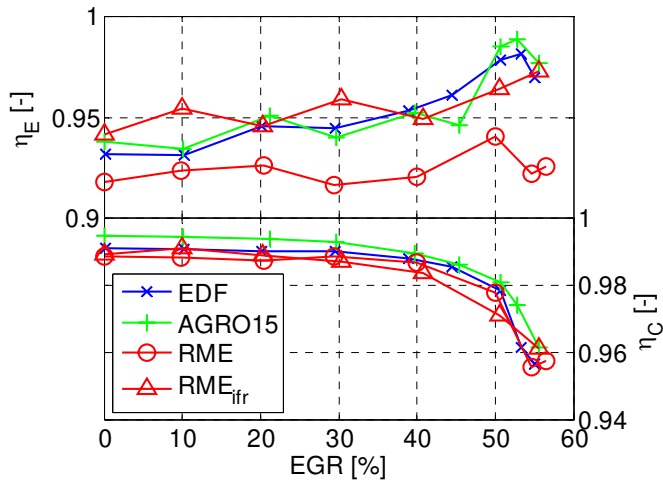
**Figure 12: $\eta_E$ and $\eta_C$ dependening on EGR, fuel type and fuelling rate**

For high EGR levels, $HR_{max}$ matched the amount of supplied fuel energy (Figure 12 – $\eta_E$). This was due to a highly premixed combustion mode with low radiative heat losses. The estimation of cylinder wall heat losses by Woschni's convective formulation does not cover radiative heat losses. Hence it is concluded, that the lower $\eta_E$ value at low EGR levels was caused by radiative heat losses due to increased local temperatures during diffusive combustion.

Presumed that the Wochni formulation comprehends convective heat losses correctly, it can be concluded that the balance between convective and radiative heat losses changes with EGR level. At low EGR, the local flame temperature increases due to less time for charge entrainment. Hence, less mass is involved with initial combustion. This gives higher local temperatures, higher NOx (see Figure 5) and more radiative heat losses.

For the RME case, two sub cases are depicted in Figure 12:

- For the standard RME case, fuelling rate was adapted to the amount of energy supplied with EDF and AGRO15, according to their LHV.

- For RME$_{ifr}$, fuel rate was increased such that engine load matched the EDF and AGRO15 cases within an accuracy of 0.2 bar IMEP.

For these two cases, a considerable difference in $\eta_E$ was observed for the whole EGR sweep, which might originate from a difference in $\eta_C$.

The point of maximum $\eta_E$ is situated at 50% EGR and is concurrent with maximum PM emissions. This shows that soot oxidation reactions abate with increasing EGR level due to decreasing local temperatures. Combustion efficiency is included in calculation of $\eta_E$. The decrease of $\eta_E$ at the highest EGR level is either due to a more effective combustion or due to an underestimation of combustion efficiency (Figure 12 – $\eta_C$). An underestimation is due to emission measurement error at instable combustion conditions.

The analysis results presented in this section lead to the following preliminary conclusions regarding measurement accuracy: HC and CO emissions are lowered with decreasing EGR. Hence, exhaust measurement errors have the strongest effect at high EGR conditions and are moreover dependent on engine load. The estimation error for $\eta_C$ is dependent on exhaust gas emissions and influences $\eta_E$. As $\eta_E$ is overly lowered for the low load RME case, it is plausible that exhaust gas emission measurement results are underestimated for this case.

A more exact investigation of the dependency between $\eta_C$ and indicated thermal efficiency (ITE) is given in the section *Thermal Efficiency* in the appendix.

**ANALYSIS RESULTS**

In this section, previously described explanation models are applied to investigate differences in combustion characteristics due to EGR, fuel type and injection pressure.

Influence of EGR and Fuel Type

Experimental results showed fuel dependent differences for engine load and exhaust emissions due to fuel type at low *EGR* levels (Figure 5). These differences are explained by comparison of *HRR* between 0 and 50% EGR. For clearness reasons, HR plots depicted in Figure 13 were synchronized at *SOC*.

As shown in Figure 13 both premixed and diffusive *HRR* is lower for the RME case. At low load conditions, RME is considered as a poorly ignitable diesel fuel [5 pg. 125ff] which is due to a high distillation middle temperature (see Figure 3): If it is assumed that the overall liquid fuel spray has to be heated until T50 to become vaporised, and if it is moreover assumed that heat capacities for both fuel types are alike, the heat needed for warming up the liquid spray phase to vaporisation conditions is higher. Due to the high distillation temperature gradient, more time is needed for vaporisation of the initial fuel fraction, which increases ignition delay somewhat.
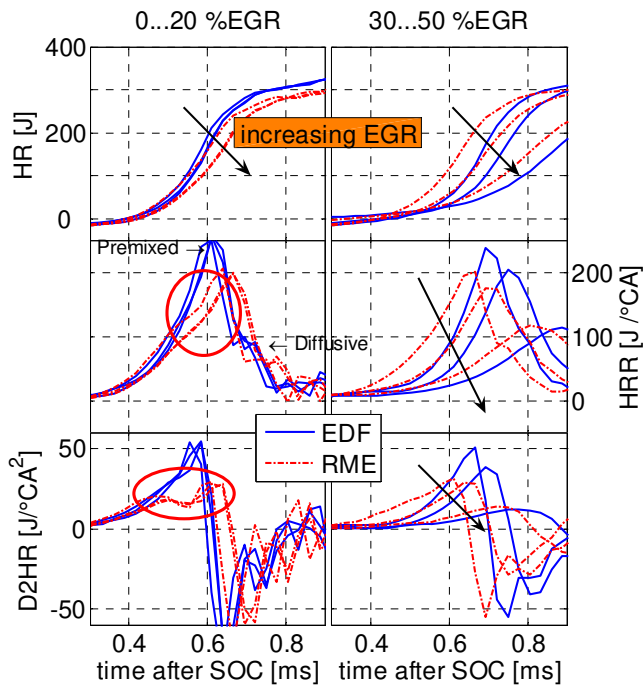
**Figure 13: Differences in HR, HRR and D2HR between EDF and RME due to EGR – *synchronized at SOC***

Due to RME's mono component like short distillation temperature interval (cf. Figure 3) a large fuel spray fraction vaporises concurrently within a small temperature and spatial interval if enough ambient heat is available. Together with a larger average droplet size due to higher fuel viscosity (Table 1, Table 5) these fuel characteristics increase the affinity of RME to form a higher amount of fuel rich reaction zones at SOC. This is reflected in a lower overall HR due to poor premixed and diffusive combustion (Figure 13 – HR).

Both overall and premixed HR is delayed for the RME case between 0...20% EGR which is in accordance with a decrease in maximum HRR (Figure 16). If EGR level is increased above 30% (Figure 13) the point of maximum HR is more delayed for the EDF case which is in contrast to the 0...20% EGR cases. This behaviour is related to the ignition delay which increases with EGR level. The time delay until auto ignition is a function of mixture quality; the ignition delay for the RME case at EGR levels above 30% is an indicator for improved mixture generation.

The ignition delay (Figure 14 – SOC-SOI) of RME was similar to EDF. For EDF, the ICN is lower than the overall CN to increase ignition delay. For RME on the other hand, the ICN is equal to the overall CN. The ICN is considered to have the strongest influence on ignition delay. Hence, the similar ignition delay between EDF and RME is related to a longer evaporation process for the RME case; more time is needed to form an ignitable fuel-air mixture.

Due to the lower energy content of RME compared to EDF, more fuel mass had to be injected to reach the same fuel energy content. Hence, the injection control

signal was lengthened from ~9.2 to ~10.0°CA, entailing a larger fuel fraction being injected after SOC (Figure 14 – SOC-EOI):
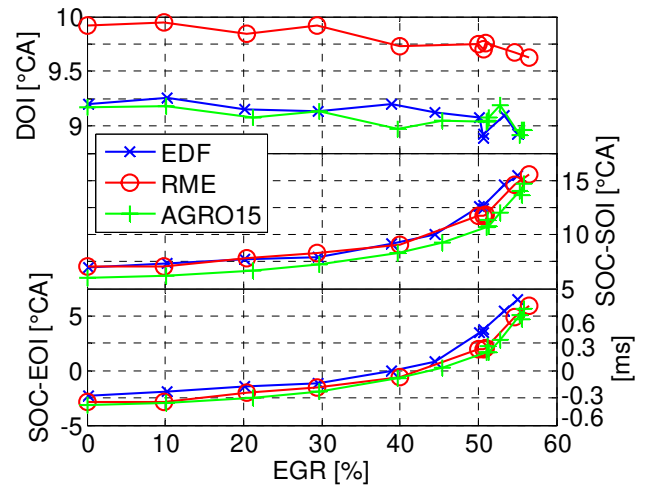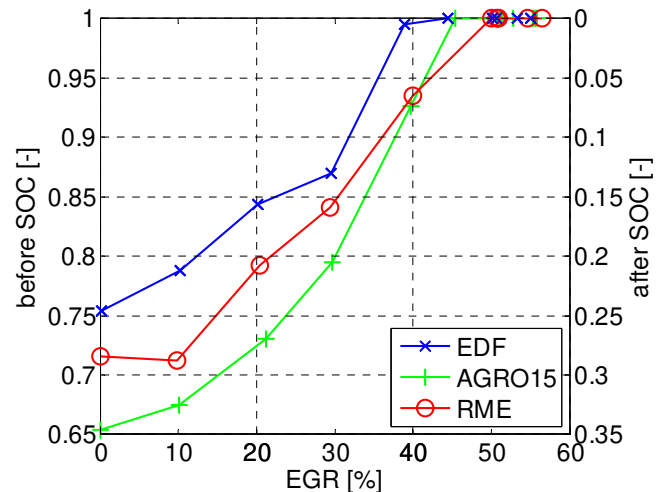


**Figure 14: Ignition delay and injection duration vs. EGR**

For RME, a slow-down in *HRR* could be observed at EGR levels between 0 and ~30% (Figure 13 - *circle*). As the EOI is situated in this region (Figure 14), it is most likely that heat losses due to fuel vaporisation are observed in the HRR. As the fuel injection mass was higher for the RME case, more heat is needed for fuel spray vaporisation.

This HRR slow-down due to EOI was coincident with increased PM level. Hence, it is most likely that early igniting fuel rich diffusive combustion zones evolving from injection during concurrent premixed combustion are the reason for increased exhaust PM.

The injection process is split into two injection fractions with help of SOC-EOI (Figure 14) as discussed before. The injected fuel mass was split into a mass fraction injected before SOC and a mass fraction injected during combustion:



**Figure 15: Injection mass ratios vs. EGR**

The injection mass ratio (Figure 15) is related to fuel dependent differences in injection mass which was adapted to keep the amount of fuel energy constant. At EGR levels beyond 45%, ignition delay is considerably increased compared to combustion without EGR. Thus, all fuel was injected well before SOC.

For the AGRO15 and the RME case a larger amount of fuel mass was injected after SOC. For AGRO15 this was due to a shorter ignition delay (Figure 14 – SOC-SOI). For the RME case, a larger fuel mass was injected entailing longer DOI and thus more fuel mass being injected after SOC.

Emission results (Figure 5) however, did not show any differences for AGRO15 in comparison to the reference fuel (EDF) whereas for the RME case differences in PM emissions were observed at low EGR conditions.

For the AGRO15 and EDF cases, concurrent fuel injection and premixed combustion was not observed in HRR. This indicates improved fuel spray evaporation due to the following properties:

- Due to low viscosity, the average spray droplet size is lower (Table 1), which improves evaporation characteristics.

- Due to a wide distillation temperature interval and a low initial distillation temperature the injected fuel spray starts to evaporate early (Figure 3).

Both factors influence the fuel spray evaporation process in a way that less spray is evaporated at a later injection stage.

In Figure 16, the maximum $HRR$ of all fuel types are compared with each other. It is observed that the maximum rate of premixed combustion is lower for both AGRO15 and RME:
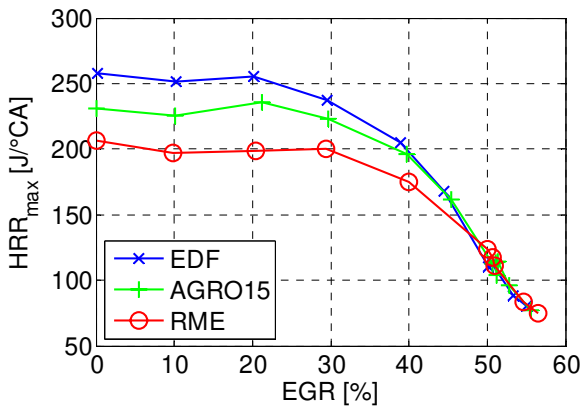


**Figure 16: Maximum HRR vs. EGR level**

The fuel dependent difference in $HRR_{max}$ is related to the vaporisation characteristics of RME. Due to an increased SMD (Table 1) less zones of air-fuel mixture close to stoichiometry are created during ignition delay which lowers premixed HRR. Fuel rich zones need more

time to mix with cylinder charge and combust at a later stage if sufficient local heat and oxygen is available for self ignition. Hence, the HR of the RME case is both delayed and decelerated due to inferior fuel spray evaporation characteristics.

If HR is separated into a diffusive and premixed HR fraction (cf. Figure 2), one obtains a different picture from what injection mass ratios (Figure 15) imply:
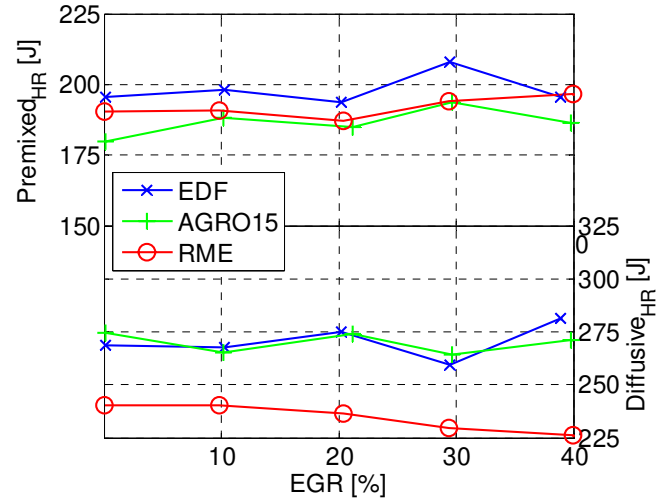


**Figure 17: HR combustion ratios in dependence of EGR**

The overall amount of heat released (Figure 17: $HR_{Diffusive}$ +$HR_{Premixed}$) is lower for the RME case even though the injection mass was chosen in a way to keep the amount of supplied fuel energy constant for all fuels.

For all cases, the premixed HR ratio is lower than the energy equivalent of the mass ratio injected before SOC. Maximum premixed HR is lowered due to the mixture generation process which takes some time and is not regarded for the estimation of injection mass ratio before and after SOC (Figure 15).

For the AGRO15 and EDF case, the diffusive HR ratio (Figure 17) is basically constant until 40% EGR. For the RME case, diffusive HR was considerably lower than is anticipated from injection mass ratio (Figure 15). This indicates poor diffusive combustion which is related to a low FCN. Moreover, a slight wear-off in diffusive HR was observed with increasing EGR levels.

For the influence of EGR on different fuel types, the following is concluded:

- For all fuels, ignition delay (Figure 14) and combustion duration is increases with EGR level. A longer ignition delay promotes mixture generation. This however was *not* reflected in the amount of premixed HR.

- For the RME case, overall HR as well as the maximum HRR is lower. For EGR levels above 30%, combustion phasing was slightly earlier than for the EDF case which was in contrary to low EGR levels.

This is an indication for an improvement in mixture generation for the RME case with higher EGR levels.

- The ignition delay was shorter for AGRO15 than for the reference fuel. HR characteristics however, were similar for both fuel types: Increased fuel mass injection after SOC was not reflected in HR, which was an indication for improved fuel spray evaporation characteristics.

Influence of Rail Pressure

The variation of rail pressure led to a further indication for the assumption of locally fuel rich combustion of RME as the source for PM. In Figure 18, fuel specific differences at diffusive-only HR are obvious. Observed differences in HR for EDF and RME were considerable:
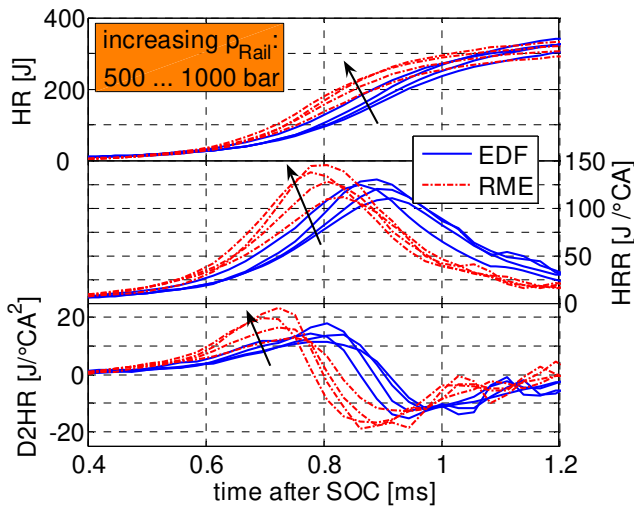


**Figure 18: Influence of injection pressure on HR (50%EGR)**

In Figure 18, a decrease in ignition delay and combustion duration is observed, while $HR_{max}$ and $HRR_{max}$ increased concurrently with higher injection pressure. Increased $HR_{max}$ is an indicator for improved mixture generation.

This indicator is strengthened by the calculation of average droplet size. In Figure 19 it is depicted, that SMD is considerably influenced by injection pressure.
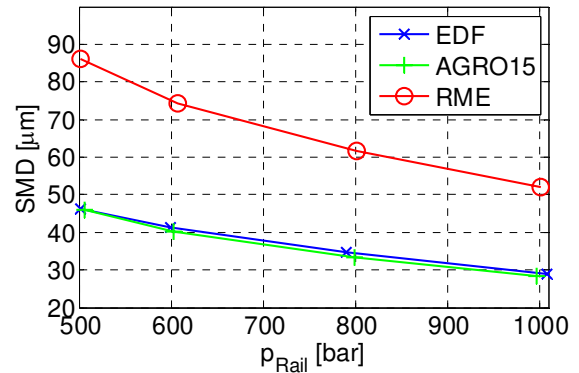


**Figure 19: SMD size reduction due to increasing injection pressure**

The injection velocity is the strongest factor influencing SMD (eq.2). Increasing injection pressure increases relative velocity between injected fuel und cylinder charge. Hence, average droplet size is reduced which improves vaporisation characteristics for all fuels. RME, however, which has the largest SMD due to higher fuel viscosity benefits strongest from increasing injection pressure which is reflected in decreasing emissions (Figure 6) and increasing $HR_{max}$ (Figure 18).

Ignition delay and combustion duration were shorter with increasing injection pressures. The shortening of ignition delay at high rail pressures was compensated by the shortening of injection duration. No considerable variation in premixed and diffusive HR was observed.

For the influence of increasing injection pressure on HR, the following is concluded:

- Average droplet size decreases with injection pressure, which improves fuel spray evaporation characteristics.

- Fuel mixture generation is improved which is reflected in improved $HR_{max}$, shorter ignition delay and shorter combustion duration.

- The fuel type RME benefits the most from increased injection pressure, which is related to a stronger reduction in SMD compared with EDF.

**CONCLUSIONS**

Measurement results from an HSDI Diesel engine were studied by detailed heat release analysis. For all fuel types, increasing EGR levels increase ignition delay (Figure 14), which improves mixture generation and premixed combustion. Increasing EGR level entails a longer premixed combustion duration (Figure 13), which lowers maximum HRR. In this way the amount of fuel rich, locally hot zones is minimised. Hence, PM emissions originating from fuel rich combustion were improved.

RME and AGRO15 showed different combustion characteristics from EDF at low load conditions which depends on the following factors:

- Injection duration was longer for the RME case due to lower fuel energy content. This resulted in less available time for fuel mixture generation; a larger fuel fraction was injected close to or after SOC.

- For RME, the high ICN resulted in early ignition of fuel rich zones entailing suboptimal premixed HR which was indicated by lower maximum HR (Figure 13).

- Due to higher fuel viscosity, SMD is increased for RME (Figure 19). Increased average droplet size increases the affinity to form locally fuel rich zones. Fuel dependent SMD differences can be compensated by increased injection pressure.

- RME combustion characteristics can be considered as poor at low load conditions. Due to a high distillation middle temperature, short distillation temperature interval (Figure 3) and increased SMD, fuel vaporisation is delayed. Premixed HR is unsteady due to concurrent fuel spray evaporation and premixed combustion (Figure 13).

- The ratio of diffusive and premixed HR is lower for RME than for the reference fuel (Figure 17). This is related to the lack of FCN improvers. The lower diffusive HR entails poor emission oxidation characteristics.

- Supplementary RME measurements with slightly increased engine load resulted in considerably improved $\eta_E$ (Figure 12) which is an indicator for a strong load dependency of $\eta_E$ at low load conditions.

- The AGRO15 and EDF case showed that shortened ignition delay, concurrent fuel mass injection and premixed combustion have minor influence on PM emissions due to good fuel spray vaporisation characteristics.

- For AGRO15, HC and CO emissions were decreased compared to RME and EDF at low load/low EGR conditions even though diffusive HR was lower (Figure 17). This indicates improved oxidation characteristics during diffusive combustion.

If alternative diesel fuels with varying properties shall be included in future emission legislations, technical possibilities exist to meet these legislations: Today's Diesel engines are equipped with advanced combustion control devices like EGR, Common Rail and Turbo Charging. In addition, fuel and/or cylinder pressure sensors open possibilities for a multi fuel production engine. If engine control strategy is adapted to a specific fuel type during operation, emission demands can be met for a variety of fuels.

## REFERENCES

1. Chang, D., Van Gerpen, J.: "Determination of Particulate and Unburned Hydrocarbon Emissions from Diesel Engines Fueled with Biodiesel", SAE 982527

2. May, H., Hattingen, U., Theobald, J., Weidmann, K., König, A.: "Untersuchung des Betriebs- und Abgasemissionsverhaltens eines Dieselmotors mit Oxidationskatalysator - Verwendung von Rapsöl-Methyl-Ester (RME)", MTZ Ausgabe Nr.: 1998-02

3. Hopp, M.: "Untersuchung des Einspritzverhaltens und des thermischen Motorprozesses bei Verwendung von Rapsöl und Rapsmethylester in einem Common-Rail-Dieselmotor", Dissertation Universität Rostock 2005

4. Egnell, R.: "Combustion Diagnostics by Means of Multizone Heat Release Analysis and NO Calculation", SAE 981424

5. Garbe, T.: "Senkung der Emissionen eines PKW mit direkteinspritzenden Dieselmotor durch Verwendung von Kraftstoffen mit abgestimmtem Siede- und Zündverhalten", Dissertation Universität Hannover 2002

6. Munack, A., Schröder, O., Stein, H., Krahl, J., Bünger, J.: "Systematische Untersuchungen der Emissionen aus der motorischen Verbrennung von RME, MK1 und DK", Landbauforschung Völkenrode – FAL Agricultural Research 2003

7. Krahl, J., Munack, A., Schröder, O., Stein, H., Bünger, J.: "Influence of Biodiesel and Different Designed Diesel Fuels on the Exhaust Gas Emissions and Health Effects", SAE 2003-01-3199

8. Taylor, J., McCormick, R., Clark, W.: "Report on relationship between molecular structure and compression ignition fuels, both conventional and HCCI", National Renewable Energy Laboratory 2004

9. Murphy, M., Taylor, J., McCormick, R.: "Compendium of Experimental Cetane Number Data", National Renewable Energy Laboratory 2004

10. Woschni, G.: "A Universally Applicable Equation for the Instantaneous Heat Transfer Coefficient in the Internal Combustion Engine", SAE 670931

11. Dec, J.E.: "A Conceptual Model of Di Diesel Combustion Based on Laser-Sheet Imaging", SAE 970873

12. Mayer, A.C.R., Czerwinski, J., Wyser, M.: "Impact of RME/Diesel Blends on Particle Formation, Particle Filtration and PAH Emissions" SAE 2005-01-1728

13. Munack, A., Krahl, J.: "Erkennung des RME-Betriebes mittels eines Biodiesel-Kraftstoffsensors" Landbauforschung Völkenrode – FAL Agricultural Research 2003

14. Young, H.D., Freedman, A.R., et al.: "University Physics" 9th edition Addison Wesley Publishing Company, Inc.

15. Valdsoo, T.: "Studier av atomiseringsfenomen under bränsleluftpreparering" STU dnr: 86-4560

16. R. L. McCormick, C. J. Tennant, R. R. Hayes, S. Black, J. Ireland, T. McDaniel, A. Williams, M. Frailey: "Regulated Emissions from Biodiesel Tested in Heavy-Duty Engines Meeting 2004 Emission Standards", SAE 2005-01-2200

17. Musculus, Mark. P. B.: "On the Correlation between NOx Emissions and the Diesel Premixed Burn", SAE 2004-01-1401

## CONTACT

Uwe Horn can be contacted via the following email address: uwe.horn@vok.lth.se

## DEFINITIONS, ACRONYMS, ABBREVIATIONS

| | |
|---|---|
| **AGRO15** | Mixture of 85%EDF, 5%RME and 10% higher alcohols |
| **COV** | Coefficient of variation |
| **DOF** | Degree of Freedom |
| **DOI** | Duration of Injection |
| **D2HR** | 2nd Heat Release derivate |
| **ECE** | Energy Consumption Efficiency |
| **EDF** | Euro Diesel Fuel |
| **EVO** | Exhaust Valve Opening |
| **FCE** | Fuel Consumption Efficiency |
| **FCN** | Final Cetane Number |
| **FSN** | Filter Smoke Number |
| **HR** | Heat Release |
| **HRR** | Rate of Heat Release |
| **HR$_{net}$** | Net Heat Release |
| **HR$_{ht}$** | Heat Release due to heat transfer |
| **HR$_{gross}$** | Gross Heat Release $$HR_{gross} = HR_{net} + HR_{ht}$$ |
| **IVC** | Intake Valve Closing |
| **ICN** | Initial Cetane Number |
| **ITE$_{gross/net}$** | Indicated Thermal Efficiency: $$ITE = \frac{W_{i,gross/net}}{\eta_C \cdot m_f \cdot LHV}$$ |
| **IFCE$_{gross/net}$** | Indicated Fuel Conversion Efficiency: $$IFCE = \frac{W_{i,gross/net}}{m_f \cdot LHV}$$ |
| **RME** | Rape Oil Methyl Ester / Biodiesel |
| **r$_{c,eff}$** | Effective compression ratio |
| **r$_{c,stat}$** | Static compression ratio |
| **SMD** | Sauter Mean Diameter |
| **SOC** | Start of Combustion |
| **SOI** | Start of Injection |
| **η$_E$** | Energy Conversion Efficiency |
| **η$_C$** | Combustion Efficiency $$\eta_C = \frac{IFCE}{ITE}$$ |

## APPENDIX

COMBUSTION CHARACTERISTIC VALUES

Emission analysis data can be used to calculate the combustion efficiency $\eta_C$ from the global air-fuel-ratio $A/F$, the emission gas mole fraction $\chi_i$, the ratio of exhaust gas products mole weights $\frac{M_i}{M_p}$ and the ratio of the lower heating values from emission gas components and fuel $\frac{LHV_i}{LHV_f}$ :

$$\eta_C = 1 - \left(1 + A/F\right) \cdot \sum_i \frac{M_i}{M_p} \frac{LHV_i}{LHV_f} \chi_i \qquad \text{(A.1)}$$

$\eta_C$ determines how effectively fuel energy is converted to heat energy. For a given load, higher combustion efficiency implies in general lower fuel consumption.

As heat losses are solely modelled by Woschnis' approach, energy conversion efficiency ($\eta_E$) is used as a measure for the quality of HR:

$$\eta_E = \frac{HR_{max}}{\dot{m}_{fuel} \cdot \eta_c \cdot LHV} \qquad \text{(A.2)}$$

$\eta_E$ makes it possible to determine how combustion mode dependent thermodynamic properties as HRR-shape, -duration and -location influence heat losses.

FUEL PROPERTIES

During engine measurements, the engine was operated under low load conditions (4 bar IMEP) with three different fuel types: Euro Diesel fuel (EDF), RME, and a mixture of 10% higher alcohols, 5% RME and 85% EDF (AGRO15)

**Table 5: Fuel Property Data**

| Parameter | EDF | RME | AGRO15 |
|---|---|---|---|
| flashpoint [°C] | 64 | >110[2] | |
| water content [ppm] | <200[1] | <300[2] | |
| density (15°C) [g/l] | 834,9 | 883[2] | 828.5 |
| kinematic viscosity [mm$^2$/s] (40°C) | 2.575 | 4.55[3] | 2.45[4] |
| kinematic viscosity [mm$^2$/s] (100°C) | 1.15[3] | 1.93[3] | 1.75[4] |
| surface tension [N/m] | ~26.5[3] | ~29[3] | 26.2[4] |
| sulfur content [ppm] | 49 | 5 | 1.7 |
| aromate content [vol%] | 18 | 0 | 4.2 |
| olefine content [vol%] | 0 | 0 | |
| parafine content [vol%] | 0 | 0 | |
| LHV [MJ/kg] | 43.15 | ~38[3] | 42.56 |
| C [mass%] | 86.37 | 77.4 | 83 |
| H [mass%] | 13.63 | 12.1 | 14.6 |
| O [mass%] | 0 | 10.5 | 2.4 |
| CN | 51.3 | 56 | 52.3 |
| ICN | 24[3] | 56[3] | |
| FCN | ~70[3] | 55[3] | |

1: EN 590
2: E DIN 51 606
3: typical analysis data
4: interpolated data from EDF, RME and Ethanol at 20°C

## ITE CALCULATIONS

If highly premixed diesel combustion is simplified as a constant volume heat release at CA50 with a constant adiabatic exponent, the difference in thermal efficiency due to combustion phasing can be approximated as:

$$\eta_T = 1 - \frac{1}{r_{c,eff}^{\kappa-1}} \tag{A.3}$$

with

$$r_{c,eff} = \begin{cases} 15.51 \text{ for } CA_{50,min} = 2.5°CA \\ 15.23 \text{ for } CA_{50,max} = 4.5°CA \end{cases} \tag{A.4}$$

and

$$\kappa = 1.37 \tag{A.5}$$

one obtains

$$\eta_T = \begin{cases} 0.6374 \text{ for } CA_{50,min} = 2.5°CA \\ 0.6349 \text{ for } CA_{50,max} = 4.5°CA \end{cases} \tag{A.6}$$

Differences in HR due to combustion phasing can not be larger than $COV(\eta_T) < 0.4\%$ which is well within the interval of $COV(IMEP) \approx 2.5\%$. Hence, changes in ITE due to combustion phasing are negligible.

## ITE AND COMBUSTION EFFICIENCY

Indicated thermal efficiency (ITE$_{gross}$ – see abbreviations) is related with $\eta_E$ (eq. A.2), but does not take exhaust flow heat losses, convective cylinder wall heat losses and pumping losses into account.

In Figure 20, considerably different trends for ITE$_{gross}$ are observed for different fuel types and load cases:
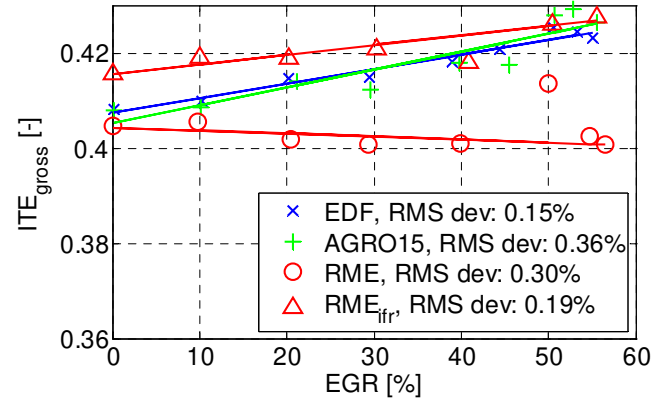


**Figure 20: Error estimation of ITE due to variation of EGR**

Figure 20 shows that ITE$_{gross}$ for the RME cases diverge from each other. The strong variation of ITE$_{gross}$ from the weighted average at high EGR levels and low injection pressures is an indication for the erroneousness of exhaust measurement at high EGR conditions. The fuel dependent measurement error increases with increasing emissions. Comparison of the RME$_{ifr}$ with the RME case (Figure 12 - $\eta_C$) shows that combustion efficiency is slightly lowered for the RME case but does not compensate the differences in ITE.

This behaviour is also observed for the $p_{Rail}$ – sweep (Figure 21): If rail pressure is increased at 50% EGR, combustion efficiency improves for the RME case which is also reflected in ITE$_{gross}$:
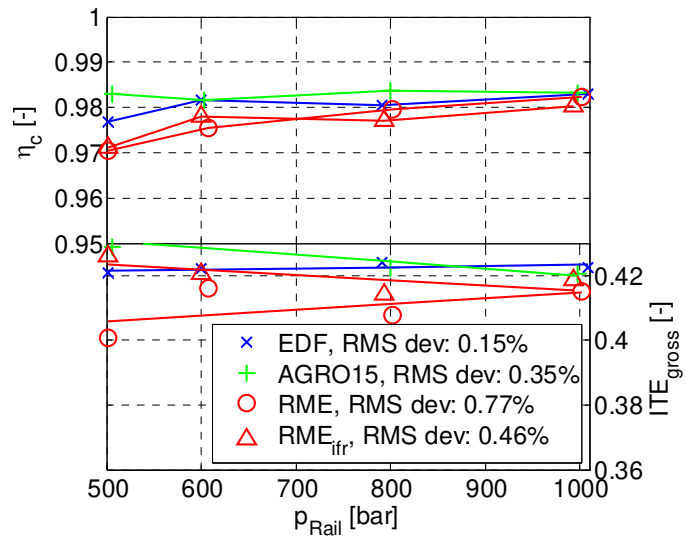


**Figure 21: Error estimation of ITE due to variation of p$_{Rail}$ (50% EGR)**

In Figure 21, ITE$_{gross}$ converges with increasing injection pressure. As ITE$_{gross}$ is reassessed regarding LHV, it should be on the same level for *all* fuel types.